



## **Magneto-chiral anisotropy: From fundamentals to perspectives**

Matteo Atzori, Cyrille Train, Elisabeth A. Hillard, N. Avarvari, Rikken G.L.J.A.

### **► To cite this version:**

Matteo Atzori, Cyrille Train, Elisabeth A. Hillard, N. Avarvari, Rikken G.L.J.A.. Magneto-chiral anisotropy: From fundamentals to perspectives. *Chirality*, 2021, 33 (12), pp.844-857. <10.1002/chir.23361>. <hal-03402567>

**HAL Id: hal-03402567**

**<https://hal.science/hal-03402567v1>**

Submitted on 25 Oct 2021

**HAL** is a multi-disciplinary open access archive for the deposit and dissemination of scientific research documents, whether they are published or not. The documents may come from teaching and research institutions in France or abroad, or from public or private research centers.

L'archive ouverte pluridisciplinaire **HAL**, est destinée au dépôt et à la diffusion de documents scientifiques de niveau recherche, publiés ou non, émanant des établissements d'enseignement et de recherche français ou étrangers, des laboratoires publics ou privés.



HAL Authorization

# Magneto-Chiral Anisotropy: from fundamentals to perspectives

Matteo Atzori,<sup>[a]</sup> Cyrille Train,<sup>[a]</sup> Elizabeth A. Hillard,<sup>[b]</sup> Narcis Avarvari,<sup>[c]</sup> Geert L. J. A. Rikken<sup>\*,[a]</sup>

[a] Dr. M. Atzori, Prof. C. Train, Dr. G. L. J. A. Rikken  
Laboratoire National des Champs Magnétiques Intenses (LNCMI)  
Univ. Grenoble Alpes, INSA Toulouse, Univ. Paul Sabatier, EMFL, CNRS, Toulouse & Grenoble, France  
E-mail: geert.rikken@lncmi.cnrs.fr

[b] Dr. E. A. Hillard  
Institute de Chimie de la Matière Condensée de Bordeaux  
CNRS, Univ. Bordeaux, Bordeaux INP, ICMCB, UMR 5026, F-33600 Pessac, France

[c] Dr. N. Avarvari  
Univ Angers, CNRS, MOLTECH-Anjou, SFR MATRIX, F-49000 Angers, France

**Abstract:** The interplay between chirality and magnetic fields gives rise to a cross effect referred to as magneto-chiral anisotropy (MChA), which can manifest itself in different physical properties of chiral magnetized materials. The first experimental demonstration of MChA was by optical means with visible light. Further optical manifestations of MChA have been evidenced across most of the electromagnetic spectrum, from terahertz to X-rays. Moreover, exploiting the versatility of molecular chemistry towards chiral magnetic systems, many efforts have been made to identify the microscopic origins of optical MChA, necessary to advance the effect towards technological applications.

In parallel, the replacement of light by electric current has allowed the observation of non-reciprocal electrical charge transport in both molecular and inorganic conductors as a result of electrical magneto-chiral anisotropy (eMChA). MChA in other domains such as sound propagation and photo- and electro-chemistry are still in their infancy, with only a few experimental demonstrations, and offer wide perspectives for further studies with potentially large impact, like the understanding of the homochirality of life. After a general introduction to magneto-chiral anisotropy, we give a complete review of all these phenomena, particularly during the last decade.

**Keywords:** chirality, coordination chemistry, magnetic fields, optical properties, dichroism, electrical conductivity

## Introduction

Chirality and magnetism are two fundamental phenomena that have fascinated chemists and physicists alike for a long time, particularly in France. Louis Pasteur was the first to search – in vain – for a link between them by studying crystallization of tartrates in a magnetic field.<sup>1</sup> Subsequently, Pierre Curie pointed out the basic symmetry aspects of chirality and magnetism, corresponding to the absences of spatial inversion symmetry and time-reversal symmetry, respectively.<sup>2</sup> His work was later further refined by DeGennes.<sup>3</sup> The symmetry requirements for any process to yield a chiral result were formulated by Barron, who realized that enantioselective effects arise when magnetic fields are combined with a phenomenon with specific symmetry properties.<sup>4,5</sup> In 1962, a first implicit prediction of a link between chirality and magnetism appeared in the form of a cross-effect between natural and magnetic optical activity (NOA and MOA, respectively), which discriminates between the two enantiomers of chiral molecules.<sup>6</sup> This was followed by an independent prediction of magneto-spatial dispersion in non-centrosymmetric crystalline materials.<sup>7</sup> This cross-effect has been called magneto-chiral anisotropy (MChA) and has been independently predicted several times.<sup>8–10</sup> These predictions have stimulated experimental activity towards dedicated setups and systems to detect and finely explore these effects, at first through optical means, and later in other domains.

After recalling the symmetry arguments underpinning MChA, we will first review the main results obtained for MChA in optical phenomena. These arguments also hold for electronic transport properties and, as described in the second part, were accordingly sought for and observed in this domain. Finally, given the generality of these arguments, MChA was evidenced or forecast for other physical phenomena. The perspectives opened by these manifestations of MChA will be presented in the final part.

## Optical MChA

Optical MChA gives us the opportunity to detail the symmetry rules underlying any MChA effect. Optical MChA can be most easily appreciated by expanding the dielectric tensor of a chiral medium subject to a magnetic field to first order in the wave vector  $\mathbf{k}$  of the light and the magnetic field  $\mathbf{B}$ , retaining all symmetry-allowed terms<sup>7</sup>:

$$\varepsilon_{ij}(\omega, \mathbf{k}, \mathbf{B}) = \varepsilon_{ij}(\omega) + \alpha_{ijl}(\omega)\mathbf{k}_l + \beta_{ijl}(\omega)\mathbf{B}_l + \gamma_{ijlm}(\omega)\mathbf{k}_l \cdot \mathbf{B}_m \quad (1)$$

For the propagation direction of the light  $\mathbf{k}$  parallel to  $\mathbf{B}$  and for high-symmetry media like gases, liquids, cubic crystals or uniaxial crystals with their optical axis parallel to  $\mathbf{B}$ , the optical eigenmodes are right- and left-handed circularly polarized waves, denoted by  $+$  and  $-$ . For such media, Eq.(1) can be simplified to<sup>7,9</sup>:

$$\varepsilon_{+/-}(\omega, \mathbf{k}, \mathbf{B}) = \varepsilon(\omega) \pm \alpha^{D/L}(\omega)\mathbf{k} \pm \beta(\omega)\mathbf{B} + \gamma^{D/L}(\omega)\mathbf{k} \cdot \mathbf{B} \quad (2)$$

where  $x^D(\omega) = -x^L(\omega)$  refers to right- ( $D$ ) and left- ( $L$ ) handed media,  $\alpha^{D/L}$  describes NOA,  $\beta$  describes MOA and  $\gamma^{D/L}$  describes MChA. From Eq. (2), it is possible to glean the essential features of MChA:

1. The scalar product underlines its dependence on the *relative* orientation of  $\mathbf{k}$  and  $\mathbf{B}$ ;
2. The  $D/L$  superscript marks its dependence on the handedness of the chiral medium, that is its *enantioselectivity*;
3. Not being sensitive to the handedness of the circularly polarized eigenmodes guarantees its *independence* from the polarization state of light.

Accordingly, as far as optics is concerned, MChA corresponds to a difference in the properties of a chiral medium in a magnetic field for unpolarized light propagating parallel or anti-parallel to the field. When related to absorption, this difference is called dichroism and thus MChA effects are often named Magneto-Chiral Dichroism (MChD).

Prior to any experimental demonstration, Baranova *et al.* were the first to present a simple microscopic model.<sup>9</sup> It is an extension of the classical Becquerel model for the Faraday effect<sup>11</sup> and it calculates MChD as the perturbation by the Larmor precession of the valence electrons on the optical activity of the medium. It predicts the MChD anisotropy factor, defined as the ratio between the difference between the absorptions for the two relative orientations of  $\mathbf{k}$  and  $\mathbf{B}$  over their sum, as:

$$g_{MChD} = g_{NCD} \cdot g_{MCD} \quad (3)$$

A detailed molecular theory for MChA in molecular liquids and gases was formulated for the first time by Barron and Vbrancich.<sup>12</sup> Ab initio calculations of MChD of simple diamagnetic molecules have completed the picture.<sup>13,14</sup>

The early predictions of this original second order effect with a relatively weak magnitude stimulated the design and construction of dedicated experimental setups able to provide unambiguous experimental proof of MChA effects. Twenty years after the theory proposed by Baranova *et al.*, the first experimental observation of MChA was reported.<sup>15</sup> The chemical system was a homoleptic tris-bischelated helical europium(III) complex where the control of the chirality was assured through the complexation of the metal ion with an enantiopure  $\beta$ -diketonate derivative of camphor, namely 3-(trifluoroacetyl)-camphorate.<sup>15</sup> The demonstration of the effect exploited the luminescent properties of the lanthanide ion. As shown in Figure 1a, the solution containing the enantiopure complex was irradiated perpendicular to the applied magnetic field. The difference in intensity for light emitted parallel and antiparallel to the magnetic field revealed the MChA. The ability to detect small MChD signals was assured by applying an oscillating magnetic field associated with a lock-in detection. The collected signal showed all the characteristics of MChA listed above with  $g_{MChD} = 3 \cdot 10^{-3} \text{ T}^{-1}$  for the  $^5D_0 \rightarrow ^7F_1$  transition at room temperature. Soon after, an interferometric setup (Figure 1b) was proposed to measure the magneto-chiral birefringence of a solution containing ( $d/l$ )-3-(trifluoroacetyl)-camphor.<sup>16</sup> Interferometry elegantly canceled out all spurious effects. The principles of this experiment were further used to detect a MChA corresponding to a  $10^{-10} \text{ T}^{-1}$  change in the refractive index of limonene.<sup>17</sup>

MChD was then demonstrated in the solid state in the  $\alpha$  phase of nickel(II) sulfate.<sup>18</sup> In this polymorph, upon spontaneous resolution, the sulfate-bridged nickel(II) ions form one dimensional (1D) helical chains thanks to the non-centrosymmetric tetrahedral shape of the sulfate anion (Figure 2a).

1. The investigation of the effect in other regions of the electromagnetic spectrum;
2. The identification of the microscopic parameters that govern the effect;
3. The exploitation of the dependence of MChD on the magnetization of the material.

As to the first objective, the largest effects are expected when the typical length of the chiral object is of the same order of magnitude as the wavelength of the probing wave. Accordingly, millimetric ferromagnetic helices were designed and used to detect MChD using microwaves.<sup>19</sup> Similarly, a millimetric chiral metamaterial consisting of a copper wire wrapped around a ferrite cylinder demonstrated a MChD response, with the prediction of a highly enhanced peak arising from a Fano resonance.<sup>20,21</sup>

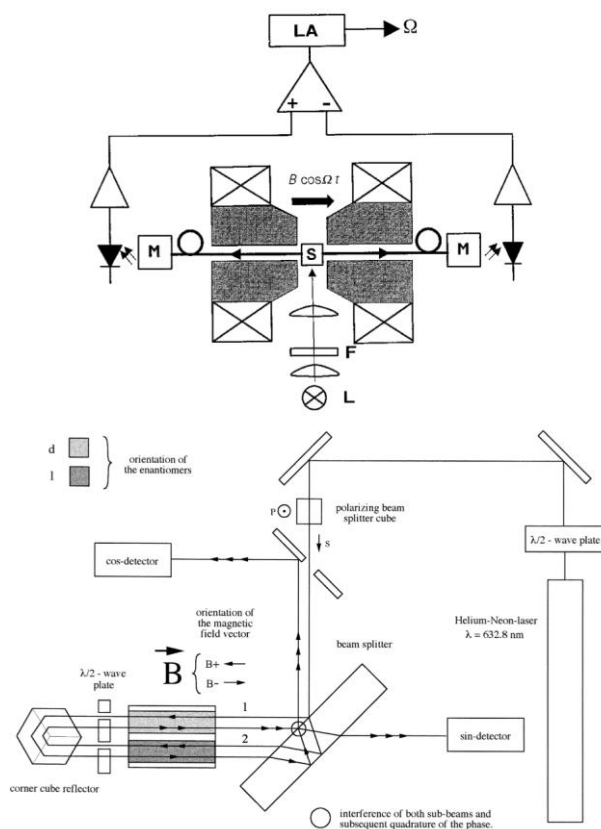


FIGURE 1 Experimental setups for measuring (top) magneto-chiral anisotropy for luminescent chiral lanthanide complexes (adapted with permission from ref. 14); (bottom) magneto-chiral birefringence for a chiral solvent. Adapted with permission from ref. 15.

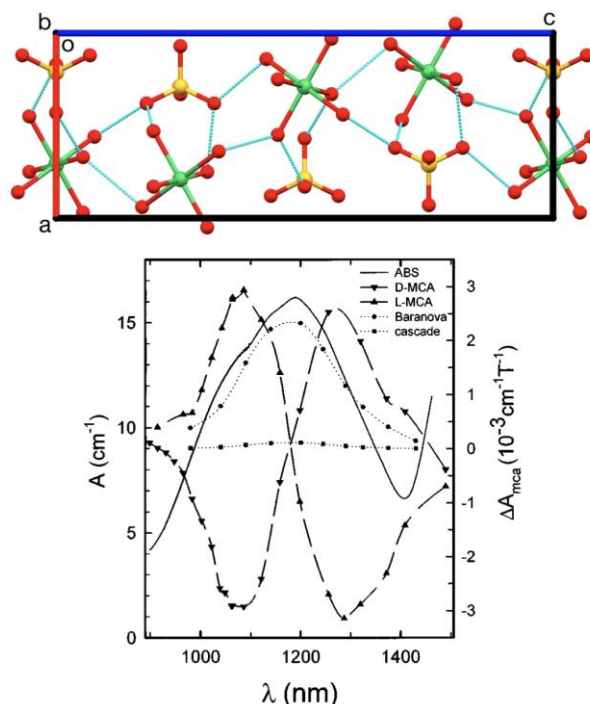


FIGURE 2 (top) Helical structure of  $\alpha$ -NiSO<sub>4</sub>·6H<sub>2</sub>O and (bottom) comparison between experimental (triangles), calculated (circles, Baranova model) and cascaded (squares) MChD. Reprinted with permission from ref. 18.

After an initial report of XMChA in chromium oxide in the XMChD-active Shubnikov group  $\bar{3}'$  in 2002,<sup>22</sup> recent years have shown a growing interest in this phenomenon, particularly in molecular systems. The first such report of XMChA in molecules was presented for powder samples of a Tb(III)Ni(II)<sub>6</sub> cluster at the Tb L<sub>2</sub>-edge, where the chirality is provided by L- or D-proline supporting ligands.<sup>24</sup> The room-temperature XMChA response was remarkably large, reaching approximately 1% of the absorption. This was attributed to strong spin-orbit coupling in the heavy lanthanide, and, notably, no XMChD could be detected at the Ni K-edge. Recently XMChA has been observed in another lanthanide compound, holmium oxydiacetate (Figure 3), at the Ho L<sub>3</sub>-edge at  $\pm 4$  T and 2.7 K.<sup>25</sup> This compound has helicoidal chirality due the wrapping of the three oxydiacetate ligands in right- and left-turning propellers and undergoes spontaneous resolution of the enantiomers upon crystallization. The XMChA response was quite weak, attributed to limited hybridization between the localized 4f orbitals and extended 5d orbitals.

The importance of magnetic anisotropy was clearly demonstrated in XMChA studies on isostructural helicoidal chains of anisotropic cobalt(II) or isotropic manganese(II) ions by Sessoli *et al.*<sup>26</sup> These compounds, [M(hfac)<sub>2</sub>NITPhOMe], consist of divalent metal centers supported by ancillary hexafluoroacetylacetonate ligands, bridged by nitronyl-nitroxide organic radicals, with chiral crystals being obtained by spontaneous resolution. While both analogues demonstrated unambiguous XNCD and XMCD, only the anisotropic Co(II) center gave rise to strong XMChD of  $g_{\text{MChD}} = 3.5\%$ , while the response of the isotropic Mn(II) center was approximately ten times weaker, even if the magnetization of the latter is higher. Interestingly, the intensity of the XMChD response of the Co(II) exceeds that of the XMCD ( $g_{\text{MCD}}$  ca. 2.7%) and XNCD ( $g_{\text{NCD}}$  ca. 3%) signals, showing that Eq. (3), which was proven to be qualitatively correct in the visible range, does not at all apply in the X-ray range.

The above examples are a clear indication of the universality of optical MChA effects and give some clues in identifying the microscopic parameters driving MChD. In the case of the [M(hfac)<sub>2</sub>NITPhOMe] compounds, the orbital contribution to the magnetic moment, which is essentially quenched in the manganese derivative, provides a straightforward experimental demonstration of the crucial role played by magnetic anisotropy in the magnitude of MChD signals in this region of the electromagnetic spectrum. On the contrary, MChD could also be observed in the visible range for chromium(III) and manganese(II) octahedral chiral centers, suggesting that orbital contributions are perhaps not so crucial for these wavelengths.<sup>27</sup> To answer this question, some of us have recently investigated the compound [Mn<sup>III</sup>(cyclam)(SO<sub>4</sub>)]ClO<sub>4</sub>·H<sub>2</sub>O (cyclam = 1,4,8,11-tetraazacyclotetradecane), which is composed of 1D helical chains featuring high spin manganese(III) centers in an elongated octahedral environment (Figure 4a) which is known to possess strong single-ion magnetic anisotropy.<sup>28</sup>

An improved experimental setup allowed a fine spectroscopic analysis of the absorption and MChD spectra in the visible and in the near infra-red (NIR) region down to 4 K. It was thus possible to identify all the electronic transitions

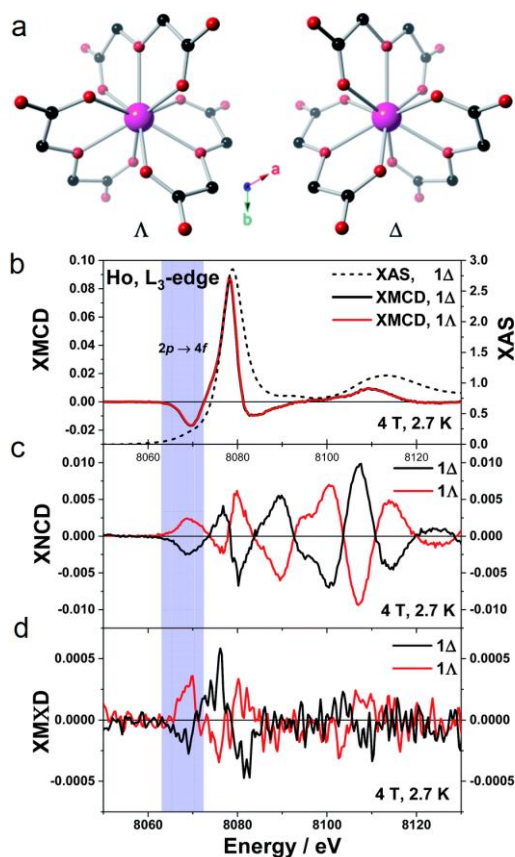


FIGURE 3 (a) Molecular representation and (b-d) X-ray dichroisms for holmium oxydiacetate at 2.7 K in a 4 T magnetic field. Adapted with permission from ref. 25.

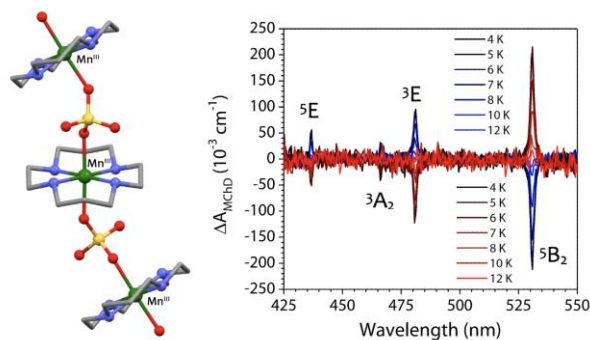


FIGURE 4 (left) Helical structure of [Mn<sup>III</sup>(cyclam)(SO<sub>4</sub>)]<sup>+</sup> and (right) experimental MChD. Adapted with permission from ref. 28.



in this compound. It appears that the transitions with a strong SOC character exhibited the most intense relative MChD signals with  $g_{MChD}$  up to  $0.13 \text{ T}^{-1}$  at 4 K (Figure 4b). This transition was one order of magnitude more intense than the most intense MChD signal for a SOC inactive transition. These results established the central role played by the orbital moment in the MChD in the visible range as previously observed in the X-ray region.

To further assess the importance of this parameter, we focused on *tris*(1,2-diaminoethane)nickel(II) and cobalt(II) complexes.<sup>29</sup> These tris(bischelated) helical complexes are obtained in their enantiomeric forms (Figure 5a) by spontaneous resolution during crystallization. Both compounds exhibit strong MChD signals corresponding to the  $d-d$  transitions of the metal ions with  $g_{MChD}$  up to  $0.19 \text{ T}^{-1}$  at 960 nm and 4 K for the cobalt(II) derivative. For the nickel(II) derivatives, the enantiopure single-crystals were measured for light propagating along the  $c$  crystallographic axis (axial configuration) or perpendicular to this axis (orthoaxial configuration) (Figure 5b). The electronic transitions are definitely the same for the two orientations but the MChD intensities vary dramatically upon rotation of the crystals, eventually changing sign for the transition observed at  $\lambda = 967 \text{ nm}$ . To fully understand these results, *ab initio* calculations were performed for the nickel(II) derivatives.

These calculations took into account the SOC coupling (indeed making them unfeasible for the  $S = 3/2$  cobalt(II) complexes) and vibronic coupling. Without this second ingredient, the spectral position of the MChD signals were essentially correct whereas the calculated intensities were not consistent with the experimental ones and no influence of relative orientation of the crystal and light wavevector could be evidenced. On the contrary, taking into account the vibration of the whole metal complex led to a quantitative agreement between the experiment and the theory for both orientations.

This study is very informative. Experimentally, the  $g_{MChD}$  are among the highest observed to date though measured on a simple paramagnet. It highlights the interest of using metal centers with high SOC character such as heavier transition metal ions or lanthanides. Moreover, the importance of vibronic coupling underlines that the flexibility of this ligand environment favors MChD effects.

As MChD intensity is proportional to the magnetization of the materials and further amplified when SOC is active, chiral lanthanide compounds are promising systems to search for high MChA effects. Reminiscent of the first experimental demonstration of MChD in the emission of a chiral  $\text{Eu}^{3+}$  complex,<sup>15</sup> Taniguchi *et al.* demonstrated a strong MChD emission in a chiral  $\text{Tb}^{3+}$  complex, dispersed in polymer films, with an luminescent dichroism of up to 16% at 14 T and 5 K.<sup>30</sup> Lanthanide ions also feature in the observed MChD response for the triple-decker  $\text{Dy}^{3+}$  complex constructed of a chiral porphyrin ligand and capped by two phthalocyanine ligands, studied in solution by Wang *et al.*<sup>31</sup> Recently, MChD detected through light absorption has been studied in helicene-based enantiopure ytterbium(III) complexes.<sup>32</sup> In this compound we combined the strong SOC of lanthanides, the magnetic dipole allowed character of the  $^2F_{5/2} \leftarrow ^2F_{7/2}$  transition, the intrinsic helical chirality of helicene-based ligands and their ability to provide a helical chirality at the lanthanide center to probe a potentially strong MChD associated to the aforementioned f-f transition. Indeed, this compound showed a strong MChD response at 4 K with  $g_{MChD}$  up to  $0.12 \text{ T}^{-1}$ , with a signal detected up to 150 K.<sup>32</sup> Interestingly, the temperature evolution of the MChD signal, that changes from an absorption-like lineshape at low temperatures to a derivative-like lineshape at high temperatures, allowed for the first time to identify and disentangle two intrinsic mechanisms at the basis of MChD in the visible range.<sup>12</sup> The former, associated with a so-called C-term, is due to the change in the population distribution of the ground state

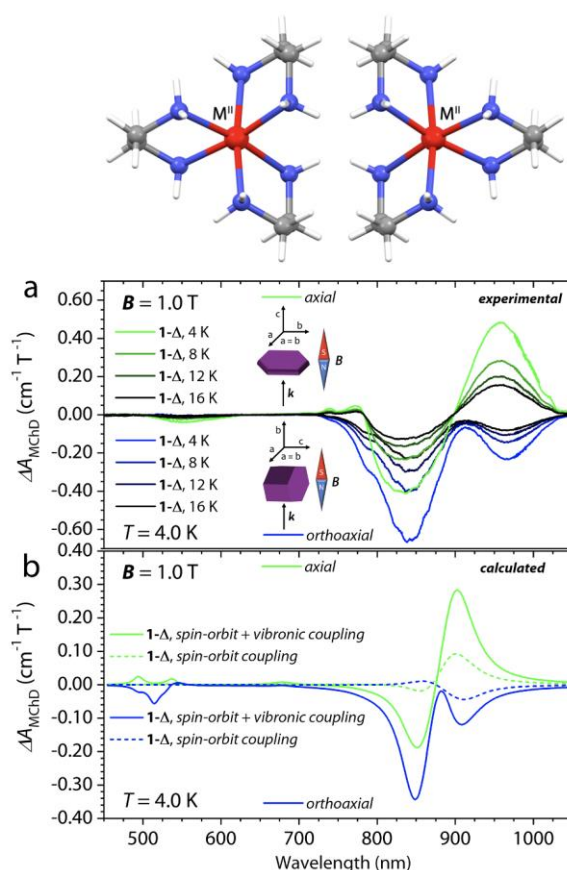


FIGURE 5 (top) The two enantiomers of tris(ethylenediamine metal(II) complexes (bottom) and experimental (upper panel) and calculated (lower panel) MChD for the nickel(II) derivative. Adapted with permission from ref. 29.

spin multiplet, while the latter, which is associated with a so-called A-term, to the lifting of the degeneracy of the ground or excited state by the magnetic field.

Some closed-shell organic compounds have also been reported to show MChD.<sup>33,34</sup> This can appear as surprising at first sight since it somehow contradicts the principles put forward in the previous systems, in particular concerning the influence of orbital contributions. Nonetheless, temperature-independent A-terms also exist for diamagnetic compounds, and can generate MChD. Moreover, a common feature of all the reported MChD-active organic molecules is their aromatic  $\pi$ -system. Accordingly, the orbital angular momentum of the  $\pi$  molecular orbitals give birth to a magnetic component and the magnitude of the magnetic quantum number increases with the size of the conjugated system. In this vein, porphyrin compounds have been the most widely studied organic compounds for MChA.<sup>33</sup> Enantiospecific supramolecular organization in solution further increased MChA. For example, helical J-aggregates of protonated meso-tetrakis(4-sulfonatophenyl)porphyrin, formed by the addition of enantiopure tartaric acid, gave rise to a single MChD signal at 490 nm, which was equally found in the NCD and MCD spectra.<sup>34</sup> In another study by the same group, J-aggregates of zinc chlorins gave rise to a MChD signal at 733 nm, corresponding, as before, to the  $\pi$ - $\pi^*$  transition.<sup>35</sup>

Given the magnitude of their magnetization below their critical temperature, compounds with 2D or 3D ferromagnetic or ferrimagnetic ordering are expected to give a strong MChD response. Because there is a relationship in the symmetry requirements for chiral and ferroelectric solids, hence an important overlap in the space groups allowing optical activity and ferroelectricity,<sup>36</sup> a benchmark approach to find candidates for MChA consists in studying some of the thousand multi-ferroics reported during the last few years. In these cases, the experiment is more complex, as it is necessary to differentiate magnetoelectric responses from magneto-chiral ones. Several theoretical and experimental MChA studies using microwaves<sup>37,38</sup> or UV-visible<sup>39–41</sup> radiation have been reported on such materials in recent years.

Given the infinite variety of available chiral organic molecules, fully molecular magnets offer many synthetic strategies towards enantiopure magnets.<sup>42</sup> Herein, we focus on those which actually led to MChD measurements. The first strategy used an enantiopure counterion to template the formation of an enantiopure, magnetic oxalate-bridged bimetallic network. The enantioselective template assembly proceeded due to the strong enantiospecific intermolecular  $\pi$ -interactions between the diimine ligands of the templating cations and the oxalate bridges of the coordination network. Unfortunately, the strongly absorbing MLCT bands of the diamagnetic counter-ion precluded any MChD measurements. The template assembly of 2D oxalate-bridged networks was more difficult, as the metal centers exhibit opposite configuration within the coordination layers and, more generally, there are no obvious intermolecular interactions between the cations and the layers. Nonetheless, using  $[\text{N}((R/S)\text{-i-Bu})\text{MePr}_2]^+$  as an enantiopure templating agent, it was possible to crystallize  $[\text{N}((R)\text{-i-Bu})\text{MePr}_2][(\Delta)\text{-Mn}(\Delta)\text{-Cr}(\text{ox})_3]$  and  $[\text{N}((S)\text{-i-Bu})\text{MePr}_2][(\Lambda)\text{-Mn}(\Lambda)\text{-Cr}(\text{ox})_3]$  as pellets well-suited for MChD measurements.<sup>43</sup> Despite the fact that only isotropic ions are present in the magnetic network, we observed a strong increase of the MChD signal when passing below the Curie temperature of this ferromagnet. To envisage any application of MChD in the optical readout of magnetic data, it is necessary to increase the Curie temperature of the chiral magnets. As far as molecule-based magnets are concerned, high  $T_C$  has been found in Prussian Blue Analogs (PBA).<sup>44</sup> The right strategy to implement chirality into PBA appeared to be the introduction of an enantiopure coligand.<sup>45</sup> Indeed,  $[\text{Mn}^{II}(\text{X-}pn\text{H})(\text{H}_2\text{O})][\text{Cr}^{III}(\text{CN})_6]\cdot\text{H}_2\text{O}$  ( $\text{X} = \text{S}, \text{R}; pn = 1,2\text{-propanediamine}$ ) is a chiral PBA that can be obtained as enantiopure single crystals suitable for MChD measurements starting from enantiopure ( $S/R$ )-1,2-propanediamine. We have measured the MChD in the two enantiomers of this compound,<sup>27</sup> and observed MChD in a ferrimagnetic phase up to 38 K. Moreover, fully exploiting the spectroscopic variations of the MChD signal, we demonstrate that the most intense MChD signal arises from the manganese(II) centers, that is, the metal ion directly coordinated to the chiral coligand. This result is in line with the result obtained in cyanido-bridged 1D coordination polymers dispersed in KBr pellets.<sup>46</sup> Using the same synthetic strategy,  $((R)\text{- or } (S)\text{-MPEA})_2\text{CuCl}_4$  (MPEA =  $\beta$ -methylphenethylamine), a two-dimensional chiral hybrid ferromagnetic perovskite, was obtained and its MChD measured below its 6 K Curie temperature.<sup>47</sup> Finally, to further enhance optical MChA, Yannopapas *et al.* have recently proposed to exploit plasmonic effects.<sup>48,49</sup> They theoretically investigated magnetic nanoparticle helices coiled around plasmonic gold nanorods, calculating very strong MChD for this system opening an avenue towards a new generation of metamaterials for optical MChA.<sup>48</sup> Such systems are promising to reach the ultimate goal of observing MChD above room temperature in order to exploit this effect for the optical readout of magnetic data.

As the existence of MChA follows from basic symmetry arguments, it has been demonstrated over the whole electromagnetic spectrum from microwaves to X-rays whatever the origin of the magnetization of the medium. Taking these arguments even further, MChA is by no means restricted to optical properties, as discussed below.

## Electrical MChA

MChA has been generalized to other manifestations, in particular to electrical charge transport.<sup>50,51</sup> Analogous to the case for optical MChA, one can deduce the existence of MChA in electrical transport by a symmetry allowed expansion of the electrical resistance  $R$  of a chiral conductor in a magnetic field  $\mathbf{B}$ :

$$R(\mathbf{B}, \mathbf{J})^{D/L} = R_0(1 + \beta \mathbf{B}^2 + \gamma^{D/L} \mathbf{B} \cdot \mathbf{J}) \quad (4)$$

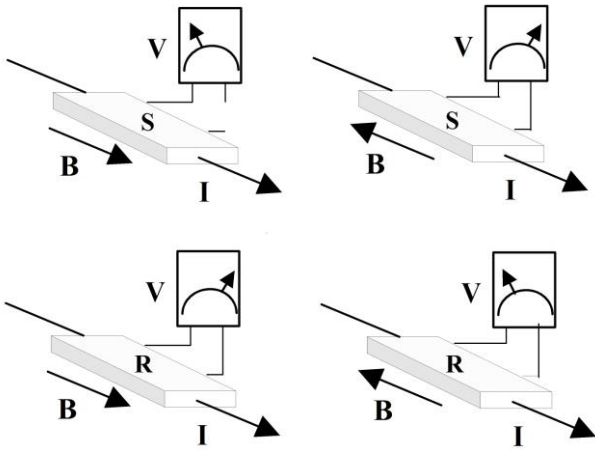


FIGURE 6 Schematic view of eMChA: the electrical resistance of the sample depends on its chirality and on the relative orientation of the magnetic field and the current.

where  $\mathbf{J}$  is the current density traversing the conductor,  $\beta$  describes the normal quadratic magneto-resistance present in all conductors, and  $\gamma^L = -\gamma^D$ . The third term on the right-hand side represents electrical MChA. By comparison with Eq. (2), it is clear that electrical and optical MChA have the same characteristics. Figure 6 schematically depicts eMChA.

Experimental verification of the validity of Eq.(4) has been obtained for metallic helices, twisted wires<sup>51</sup> and carbon nanotubes,<sup>52,53</sup> and more recently on bulk chiral organic conductors,<sup>50</sup> inorganic semiconductors,<sup>54</sup> superconducting  $\text{WS}_2$  nanotubes<sup>55</sup> and chiral magnetic metals like  $\text{MnSi}$ <sup>56</sup> and  $\text{CrNb}_3\text{S}_6$ .<sup>57</sup> Note that in the two latter cases, MChA was proportional to the magnetization of the samples.

Table 1 summarizes the reported results on eMChA.

Material	$\gamma$ ( $\text{m}^2/\text{TA}$ )	Ref.	Remark
t-Te	$10^{-8}$	54	300 K
Bi helix	$3 \times 10^{-10}$	51	77 K
$(\text{DM-EDT-TTF})_2\text{ClO}_4$	$10^{-10}$	50	300 K
MnSi	$3 \times 10^{-12}$	56	Low $T$ , magnetic
$\text{CrNb}_3\text{S}_6$	$10^{-12}$	57	Low $T$ , magnetic
SWCNT	$10^{-14}$	52	4 K

TABLE 1. Summary of reported eMChA values.

In spite of the relatively large number of reported chiral tetrathiafulvalene (TTF) derivatives,<sup>58,59</sup> only one example of crystalline molecular conductors showing eMChA has been described so far.<sup>50</sup> It involves the two enantiomers (*S,S*) and (*R,R*) of the mixed-valent radical cation salts  $(\text{DM-EDT-TTF})_2\text{ClO}_4$  (DM-EDT-TTF = dimethyl-ethylenedithio-tetrathiafulvalene) (Figure 7) which crystallize in the enantiomorphic space groups  $P6_222$  and  $P6_422$ , respectively. Both compounds, obtained by electrocrystallization, show metal like behavior in the high temperature regime, with room temperature conductivity values between 10 and 20  $\text{S cm}^{-1}$ , and metal to insulator (MI) transitions around 40 K. The eMChA effect was measured at room temperature, i.e. in the metallic regime, and the anisotropy factors were found to be equal in magnitude for the two enantiomers, but positive for (*S,S*) and negative for (*R,R*) (Figure 7). The relatively large value of the eMChA effect in these crystalline molecular conductors is probably related, among other factors, to the enantiomorphic nature of the crystal packing. For example, attempts to detect the effect in the case of semiconducting  $(\text{TM-BEDT-TTF})_2\text{SbF}_6$  (TM-BEDT-TTF = tetramethyl-bis(ethylenedithio)-tetrathiafulvalene) radical cation salts, which crystallize in the triclinic space group  $P1$ , with no chiral signature besides the absence of the inversion center, did not allow any observation of eMChA, its magnitude being beyond the limits of our experimental setup.<sup>60</sup>



These results open the possibility to perform enantioselective measurements in magnetic fields using electrical techniques that so far are insensitive to chirality, like scanning tunneling probe spectroscopy, point contact spectroscopy or electron loss spectroscopy. Note that other reports claiming electrical MChA have been published, concerning systems that are non-centrosymmetric but not chiral and that show non-reciprocal resistance with respect to a magnetic field.<sup>61,62</sup>

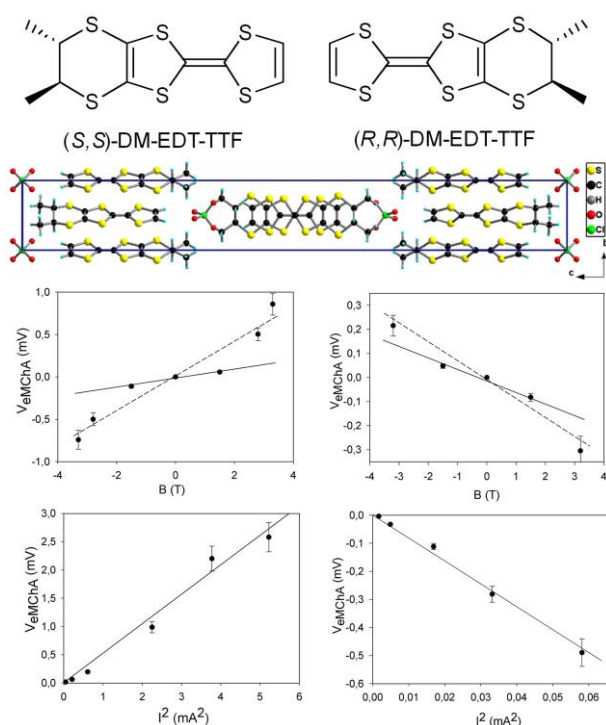


FIGURE 7 Enantiopure DM-EDT-TTF donors (top); packing diagram in the  $bc$  plane for the solid state structure of  $[(S,S)\text{-DM-EDT-TTF}]_2\text{ClO}_4$  (middle); eMChA measured on a single crystal of  $[(S,S)\text{-DM-EDT-TTF}]_2\text{ClO}_4$  (bottom left) and a single crystal of  $[(R,R)\text{-DM-EDT-TTF}]_2\text{ClO}_4$  (bottom right) showing the odd dependence of the effect on the magnetic field and the quadratic dependence of the heterodyne voltage on the current, which translates to a linear current dependence of the eMChA. Adapted with permission from ref. 50.

with  $\mathbf{k}$  and  $-\mathbf{k}$  in the presence of a magnetic field. Through the Boltzmann formalism, this then leads to an expression for the bulk conductivity that is equivalent to Eq. 4 and which predicts the correct temperature dependence and order of magnitude of the effect.<sup>54</sup> The experimental results for  $\text{MnSi}$ <sup>56</sup> are well explained by a chiral spin-cluster scattering model.<sup>65</sup>

## Other manifestations of MChA

**Sound propagation.** The symmetry arguments for the existence of MChA applies equally to the propagation of sound waves or phonons. MChA was observed in the sound velocity in the chiral ferrimagnet  $\text{Cu}_2\text{OSeO}_3$ ,<sup>66</sup> and quantitatively explained through a hybridization of magnons and phonons. A strong phonon MChA effect is predicted to exist in chiral Weyl semimetals.<sup>67</sup>

**Photochemistry.** After the first demonstration of enantio-selective photochemistry based on MChA in chromium oxalate complexes,<sup>68</sup> helical polydiacetylene was photochemically synthesized using linearly polarized light in a magnetic field.<sup>69</sup> These demonstrations call for further developments, in particular for biologically relevant molecules, to assess if MChA could be at the origin of homochirality of life on earth.

**Electrochemistry.** Another form of MChA has been observed in the electro-deposition of thin films with the current parallel to an external magnetic field. For the case of copper, silver and polyaniline, the resulting films show an enantioselectivity in their redox behavior towards chiral molecules that depends on the direction of the magnetic field during their deposition, confirming the chiral character of the deposited films, although a direct demonstration of the chirality of these films is still to be provided. The deposition process therefore shows MChA, the detailed microscopic mechanism proposed being magneto-hydrodynamical.<sup>70</sup>

A symmetry-allowed expansion can also be made for the transmission probability of spin polarized electrons through chiral molecules, leading to a spin-filtering effect referred to as chirality induced spin selectivity (CISS):

$$T(\mathbf{S}, \mathbf{I})^{D/L} = T_0(1 + \beta \mathbf{B}^2 + \Omega^{D/L} \mathbf{S} \cdot \mathbf{I}) \quad (5)$$

where  $\mathbf{S}$  is the electron spin and  $\mathbf{I}$  the electron charge current. This expansion is formally equivalent to Eq. (4), the electron spin playing the role of the magnetization, either intrinsic or induced by an external magnetic field. Surprisingly large effects have been reported for electron transport over short distances (typically nanometers) (for recent reviews, see ref. <sup>63,64</sup>).

The theoretical aspects of eMChA have been less well developed than those of the optical case. A quantitative model that reasonably agrees with the experimental data is that for trigonal tellurium, where the chirality of the crystal lattice and the absence of time-reversal symmetry at the H point in the band structure allow for the existence of linear  $\mathbf{k}$  terms in the band structure. These terms lead to the lifting of the energy degeneracy between valence band states

*Inverse MChA.* Very general thermo-dynamical arguments predict that MChA should also have an inverse counterpart, corresponding to a magnetization that is generated by an unpolarized flux through a chiral medium. This was first detailed for the optical case by Wagnière, calculating the enantioselective magnetization induced in a chiral molecular medium by an unpolarized light beam.<sup>71</sup> This effect has so far not been observed experimentally and appears as an appealing perspective for experimentalists. The electrical equivalent, a longitudinal magnetization induced by an electrical current through a chiral conductor was calculated<sup>72,73</sup> and observed in the chiral semiconductor tellurium<sup>74</sup> and in the chiral magnetic metal CrNb<sub>3</sub>S<sub>6</sub>.<sup>75</sup>

Another form of inverse MChA was reported recently, whereby a chiral spin structure was induced in the itinerant helimagnet MnP by passing an electric current parallel to a magnetic field, the handedness of which depended on the relative orientation of current and field.<sup>76</sup>

## Perspectives

Because of the generality of the symmetry arguments underpinning the phenomena combining chirality and magnetism, the last decade has seen a strongly increased interest in these manifestations and their generalization beyond optical phenomena, both among chemists and physicists. Our quantitative understanding of the optical phenomenon, although progressing, is still far from complete. Nonetheless, these efforts have allowed an increase the magnitude of MChA and have reinforced the motivation towards technological applications of optical MChA. Indeed, although MChA was initially thought to be a weak effect, recent observations of strong relative optical anisotropies in paramagnetic systems at low temperatures, or in ferro/ferromagnetic systems, suggest that materials could exist that show MChA strengths that allow for practical applications, e.g. optical diodes or optical data storage with unpolarized light.

Given the large choice of available chiral molecular conductors,<sup>58,59</sup> intensive endeavors towards the observation of eMChA and inverse eMChA in semiconducting, metallic and superconducting regimes will allow for a better understanding of the microscopic mechanisms of these phenomena depending on the nature of the chiral material.

For the other MChA phenomena, the explanations often remain hypothetical and/or qualitative, calling for further detailed studies to clearly identify, quantify and optimize the parameters that govern MChA effects. Finally, several predicted manifestations of MChA still remain to be observed e.g. in molecular diffusion or heat transport.

## Acknowledgements

This work was supported by the National Agency for Research (ANR) through the PRC 15-CE29-0006-01 (ChiraMolCo), PRC 20-CE06-0023-01 (SECRETS), PRC 19CE09-0018 (MaChiNaCo), PRC 18-CE09-0032 (MONAFER), the CNRS and the Universities of Angers, Bordeaux and the Université Grenoble Alpes. We would like to gratefully acknowledge all the collaborators who have contributed to the works described here.

## REFERENCES AND NOTES

- (1) Mason S F, *From Pasteur to Parity Non-Conservation: Theories of the Origin of Molecular Chirality*, in *Circular Dichroism*, 2nd Ed.; Berova, N., Nakanishi, K., Woody, R. W., Eds.; Wiley-VCH Verlag GmbH & Co. KGaA: New York, New York, USA, 1994;
- (2) Curie P, Sur La Symétrie Dans Les Phénomènes Physiques, Symétrie d'un Champ Électrique et d'un Champ Magnétique. *J. Phys. Théorique Appliquée* 1894;3:393–415.
- (3) De Gennes P G, Pierre Curie and the Role of Symmetry in Physical Laws. *Ferroelectrics* 1982;40(1):125–129.
- (4) Barron L D, True and False Chirality and Absolute Asymmetric Synthesis. *J. Am. Chem. Soc.* 1986;108(18):5539–5542.
- (5) Barron L D, Can a Magnetic Field Induce Absolute Asymmetric Synthesis? *Science* 1994;266(5190):1491–1492.
- (6) Groenewege M P, A Theory of Magneto-Optical Rotation in Diamagnetic Molecules of Low Symmetry. *Mol. Phys.* 1962;5(6):541–563.
- (7) Portigal D L, Burstein E, Magneto-Spatial Dispersion Effects on the Propagation of Electro-Magnetic Radiation in Crystals. *J. Phys. Chem. Solids* 1971;32(3):603–608.
- (8) Baranova N B, Bogdanov Y V, Zel'Dovich B Y, Electrical Analog of the Faraday Effect and Other New Optical Effects in Liquids. *Opt. Commun.* 1977;22(2):243–247.

- (9) Baranova N B, Zel'Dovich B Y, Theory of a New Linear Magnetorefractive Effect in Liquids. *Mol. Phys.* 1979;38(4):1085–1098.
- (10) Wagnière G, Meier A, The Influence of a Static Magnetic Field on the Absorption Coefficient of a Chiral Molecule. *Chem. Phys. Lett.* 1982;93(1):78–81.
- (11) Landau L D, Lifshitz E M, Electrostatics of Dielectrics. In *Electrodynamics of Continuous Media*; Elsevier, 1984;
- (12) Barron L D, Vrbancich J, Magneto-Chiral Birefringence and Dichroism. *Mol. Phys.* 1984;51(3):715–730.
- (13) Coriani S, Pecul M, Rizzo A, Jørgensen P, Jaszuński M, Ab Initio Study of Magnetochiral Birefringence. *J. Chem. Phys.* 2002;117(14):6417–6428.
- (14) Jansík B, Rizzo A, Frediani L, Ruud K, Coriani S, Combined Density Functional/Polarizable Continuum Model Study of Magnetochiral Birefringence: Can Theory and Experiment Be Brought to Agreement? *J. Chem. Phys.* 2006;125(23):234105.
- (15) Rikken G L J A, Raupach E, Observation of Magneto-Chiral Dichroism. *Nature* 1997;390(6659):493–494.
- (16) Kleindienst P, Wagnière G H, Interferometric Detection of Magnetochiral Birefringence. *Chem. Phys. Lett.* 1998;288(1):89–97.
- (17) Vallet M, Ghosh R, Le Floch A, Ruchon T, Bretenaker F, Thépot J-Y, Observation of Magnetochiral Birefringence. *Phys. Rev. Lett.* 2001;87(18):183003.
- (18) Rikken G L J A, Raupach E, Pure and Cascaded Magnetochiral Anisotropy in Optical Absorption. *Phys. Rev. E* 1998;58(4):5081–5084.
- (19) Tomita S, Kurosawa H, Ueda T, Sawada K, Metamaterials with Magnetism and Chirality. *J. Phys. D. Appl. Phys.* 2018;51(8):083001.
- (20) Tomita S, Sawada K, Porokhnyuk A, Ueda T, Direct Observation of Magnetochiral Effects through a Single Metamolecule in Microwave Regions. *Phys. Rev. Lett.* 2014;113(23):235501.
- (21) Tomita S, Sawada K, Kurosawa H, Ueda T, Magnetochiral Metamolecules for Microwaves. In *Springer Series in Materials Science*; 2019;
- (22) Goulon J, Rogalev A, Wilhelm F, Goulon-Ginet C, Carra P, Cabaret D, Brouder C, X-Ray Magnetochiral Dichroism: A New Spectroscopic Probe of Parity Nonconserving Magnetic Solids. *Phys. Rev. Lett.* 2002;88(23):237401.
- (23) Ascher E, Relativistic Symmetries and Lower Bounds for the Magneto-Electric Susceptibility and the Ratio of Polarization to Magnetization in a Ferromagneto-Electric Crystal. *Phys. status solidi* 1974;65(2):677–688.
- (24) Ceolín M, Goberna-Ferrón S, Galán-Mascarós J R, Strong Hard X-Ray Magnetochiral Dichroism in Paramagnetic Enantiopure Molecules. *Adv. Mater.* 2012;24(23):3120–3123.
- (25) Mitcov D, Platunov M, Buch C D, Reinholdt A, Døssing A R, Wilhelm F, Rogalev A, Piligkos S, Hard X-Ray Magnetochiral Dichroism in a Paramagnetic Molecular 4f Complex. *Chem. Sci.* 2020;11(31):8306–8311.
- (26) Sessoli R, Boulon M-E, Caneschi A, Mannini M, Poggini L, Wilhelm F, Rogalev A, Strong Magneto-Chiral Dichroism in a Paramagnetic Molecular Helix Observed by Hard X-Rays. *Nat. Phys.* 2015;11(1):69–74.
- (27) Atzori M, Breslavetz I, Paillot K, Inoue K, Rikken G L J A, Train C, A Chiral Prussian Blue Analogue Pushes Magneto-Chiral Dichroism Limits. *J. Am. Chem. Soc.* 2019;141(51):20022–20025.
- (28) Atzori M, Santanni F, Breslavetz I, Paillot K, Caneschi A, Rikken G L J A, Sessoli R, Train C, Magnetic Anisotropy Drives Magnetochiral Dichroism in a Chiral Molecular Helix Probed with Visible Light. *J. Am. Chem. Soc.* 2020;142(32):13908–13916.
- (29) Atzori M, Ludowieg H, Cortijo M, Breslavetz I, Paillot K, Rosa P, Train C, Autschbach J, Hillard E A, Rikken G L J A, Validation of Microscopic Magneto-Chiral Dichroism Theory. *Sci. Adv.* 2021;7:eabg2859.
- (30) Taniguchi K, Nishio M, Kishiue S, Huang P-J, Kimura S, Miyasaka H, Strong Magnetochiral Dichroism for Visible Light Emission in a Rationally Designed Paramagnetic Enantiopure Molecule. *Phys. Rev. Mater.* 2019;3(4):045202.
- (31) Wang K, Ma F, Qi D, Chen X, Chen Y, Chen Y-C, Sun H-L, Tong M-L, Jiang J, Chiral Bis(Phthalocyaninato) Terbium Double-Decker Compounds with Enhanced Single-Ion Magnetic Behavior. *Inorg. Chem. Front.* 2018;5(4):939–943.
- (32) Atzori M, Dhbaibi K, Douib H, Grasser M, Dorcet V, Breslavetz I, Paillot K, Cador O, Rikken G L J A, Le Guennic B, Crassous J, Pointillart F, Train C, Helicene-Based Ligands Enable Strong Magneto-Chiral Dichroism in a Chiral Ytterbium Complex. *J. Am. Chem. Soc.* 2021;143(7):2671–2675.
- (33) Ishii K, Hattori S, Kitagawa Y, Recent Advances in Studies on the Magneto-Chiral Dichroism of Organic Compounds. *Photochem. Photobiol. Sci.* 2020;19(1):8–19.
- (34) Kitagawa Y, Segawa H, Ishii K, Magneto-Chiral Dichroism of Organic Compounds. *Angew. Chemie Int. Ed.* 2011;50(39):9133–9136.
- (35) Kitagawa Y, Miyatake T, Ishii K, Magneto-Chiral Dichroism of Artificial Light-Harvesting Antenna. *Chem. Commun.* 2012;48(42):5091.

- (36) Halasyamani P S, Poeppelmeier K R, Noncentrosymmetric Oxides. *Chem. Mater.* 1998;10(10):2753–2769.
- (37) Mochizuki M, Microwave Magnetochiral Effect in Cu<sub>2</sub>OSeO<sub>3</sub>. *Phys. Rev. Lett.* 2015;114:197203.
- (38) Okamura Y, Kagawa F, Seki S, Kubota M, Kawasaki M, Tokura Y, Microwave Magnetochiral Dichroism in the Chiral-Lattice Magnet Cu<sub>2</sub>OSeO<sub>3</sub>. *Phys. Rev. Lett.* 2015;114(19):197202.
- (39) Yokosuk M O, Kim H-S, Hughey K D, Kim J, Stier A V., O'Neal K R, Yang J, Crooker S A, Haule K, Cheong S-W, Vanderbilt D, Musfeldt J L, Nonreciprocal Directional Dichroism of a Chiral Magnet in the Visible Range. *npj Quantum Mater.* 2020;5(1):20.
- (40) Sato T, Abe N, Kimura S, Tokunaga Y, Arima T, Magnetochiral Dichroism in a Collinear Antiferromagnet with No Magnetization. *Phys. Rev. Lett.* 2020;124(21):217402.
- (41) Nakagawa N, Abe N, Toyoda S, Kimura S, Zaccaro J, Gautier-Luneau I, Luneau D, Kousaka Y, Sera A, Sera M, Inoue K, Akimitsu J, Tokunaga Y, Arima T, Magneto-Chiral Dichroism of CsCuCl<sub>3</sub>. *Phys. Rev. B* 2017;96(12):121102.
- (42) Train C, Gruselle M, Verdaguer M, The Fruitful Introduction of Chirality and Control of Absolute Configurations in Molecular Magnets. *Chem. Soc. Rev.* 2011;40(6):3297.
- (43) Train C, Gheorghe R, Krstic V, Chamoreau L-M, Ovanesyan N S, Rikken G L J A, Gruselle M, Verdaguer M, Strong Magneto-Chiral Dichroism in Enantiopure Chiral Ferromagnets. *Nat. Mater.* 2008;7(9):729–734.
- (44) Verdaguer M, Bleuzen A, Marvaud V, Vaissermann J, Seuleiman M, Desplanches C, Scullier A, Train C, Garde R, Gelly G, Lomenech C, Rosenman I, Veillet P, Cartier C, Villain F, Molecules to Build Solids: High T<sub>c</sub> Molecule-Based Magnets by Design and Recent Revival of Cyano Complexes Chemistry. *Coord. Chem. Rev.* 1999;190–192:1023–1047.
- (45) Inoue K, Kikuchi K, Ohba M, Ōkawa H, Structure and Magnetic Properties of a Chiral Two-Dimensional Ferrimagnet with T<sub>c</sub> of 38 K. *Angew. Chemie Int. Ed.* 2003;42(39):4810–4813.
- (46) Taniguchi K, Kishiue S, Kimura S, Miyasaka H, Local-Site Dependency of Magneto-Chiral Dichroism in Enantiopure One-Dimensional Copper(II)–Chromium(III) Coordination Polymers. *J. Phys. Soc. Japan* 2019;88(9):093708.
- (47) Sun B, Liu X-F, Li X-Y, Zhang Y, Shao X, Yang D, Zhang H-L, Two-Dimensional Perovskite Chiral Ferromagnets. *Chem. Mater.* 2020;32(20):8914–8920.
- (48) Yannopapas V, Vanakaras A G, Strong Magnetochiral Dichroism in Suspensions of Magnetoplasmonic Nanohelices. *ACS Photonics* 2015;2(8):1030–1038.
- (49) Yannopapas V, Magnetochirality in Hierarchical Magnetoplasmonic Clusters. *Solid State Commun.* 2015;217:47–52.
- (50) Pop F, Auban-Senzier P, Canadell E, Rikken G L J A, Avarvari N, Electrical Magnetochiral Anisotropy in a Bulk Chiral Molecular Conductor. *Nat. Commun.* 2014;5(1):3757.
- (51) Rikken G L J A, Fölling J, Wyder P, Electrical Magnetochiral Anisotropy. *Phys. Rev. Lett.* 2001;87(23):236602.
- (52) Krstić V, Roth S, Burghard M, Kern K, Rikken G L J A, Magneto-Chiral Anisotropy in Charge Transport through Single-Walled Carbon Nanotubes. *J. Chem. Phys.* 2002;117:11315–11319.
- (53) Wei J, Shimogawa M, Wang Z, Radu I, Dormaier R, Cobden D H, Magnetic-Field Asymmetry of Nonlinear Transport in Carbon Nanotubes. *Phys. Rev. Lett.* 2005;95(25):256601.
- (54) Rikken G L J A, Avarvari N, Strong Electrical Magnetochiral Anisotropy in Tellurium. *Phys. Rev. B* 2019;99(24):245153.
- (55) Qin F, Shi W, Ideue T, Yoshida M, Zak A, Tenne R, Kikitsu T, Inoue D, Hashizume D, Iwasa Y, Superconductivity in a Chiral Nanotube. *Nat. Commun.* 2017;8(1):14465.
- (56) Yokouchi T, Kanazawa N, Kikkawa A, Morikawa D, Shibata K, Arima T, Taguchi Y, Kagawa F, Tokura Y, Electrical Magnetochiral Effect Induced by Chiral Spin Fluctuations. *Nat. Commun.* 2017;8(1):866.
- (57) Aoki R, Kousaka Y, Togawa Y, Anomalous Nonreciprocal Electrical Transport on Chiral Magnetic Order. *Phys. Rev. Lett.* 2019;122(5):057206.
- (58) Avarvari N, Wallis J D, Strategies towards Chiral Molecular Conductors. *J. Mater. Chem.* 2009;19(24):4061.
- (59) Pop F, Zigon N, Avarvari N, Main-Group-Based Electro- and Photoactive Chiral Materials. *Chem. Rev.* 2019;119(14):8435–8478.
- (60) Yang S, Pop F, Melan C, Brooks A C, Martin L, Horton P, Auban-Senzier P, Rikken G L J A, Avarvari N, Wallis J D, Charge Transfer Complexes and Radical Cation Salts of Chiral Methylated Organosulfur Donors. *CrystEngComm* 2014;16(19):3906.
- (61) Ando F, Miyasaka Y, Li T, Ishizuka J, Arakawa T, Shiota Y, Moriyama T, Yanase Y, Ono T, Observation of Superconducting Diode Effect. *Nature* 2020;584(7821):373–376.

- (62) Wakatsuki R, Saito Y, Hoshino S, Itahashi Y M, Ideue T, Ezawa M, Iwasa Y, Nagaosa N, Nonreciprocal Charge Transport in Noncentrosymmetric Superconductors. *Sci. Adv.* 2017;3(4):e1602390.
- (63) Yang S-H, Naaman R, Paltiel Y, Parkin S S P, Chiral Spintronics. *Nat. Rev. Phys.* 2021;3(5):328–343.
- (64) Naaman R, Paltiel Y, Waldeck D H, Chiral Molecules and the Electron Spin. *Nat. Rev. Chem.* 2019;3(4):250–260.
- (65) Ishizuka H, Nagaosa N, Anomalous Electrical Magnetochiral Effect by Chiral Spin-Cluster Scattering. *Nat. Commun.* 2020;11(1):2986.
- (66) Nomura T, Zhang X-X, Zherlitsyn S, Wosnitza J, Tokura Y, Nagaosa N, Seki S, Phonon Magnetochiral Effect. *Phys. Rev. Lett.* 2019;122(14):145901.
- (67) Sengupta S, Lhachemi M N Y, Garate I, Phonon Magnetochiral Effect of Band-Geometric Origin in Weyl Semimetals. *Phys. Rev. Lett.* 2020;125(14):146402.
- (68) Rikken G L J A, Raupach E, Enantioselective Magnetochiral Photochemistry. *Nature* 2000;405(6789):932–935.
- (69) Xu Y, Yang G, Xia H, Zou G, Zhang Q, Gao J, Enantioselective Synthesis of Helical Polydiacetylene by Application of Linearly Polarized Light and Magnetic Field. *Nat. Commun.* 2014;5(1):5050.
- (70) Mogi I, Watanabe K, Chiral Recognition of Magneto-Electropolymerized Polyaniline Film Electrodes. *Sci. Technol. Adv. Mater.* 2006;7(4):342–345.
- (71) Wagnière G, Inverse Magnetochiral Birefringence. *Phys. Rev. A* 1989;40(5):2437–2440.
- (72) Yoda T, Yokoyama T, Murakami S, Current-Induced Orbital and Spin Magnetizations in Crystals with Helical Structure. *Sci. Rep.* 2015;5(1):12024.
- (73) Yoda T, Yokoyama T, Murakami S, Orbital Edelstein Effect as a Condensed-Matter Analog of Solenoids. *Nano Lett.* 2018;18(2):916–920.
- (74) Furukawa T, Shimokawa Y, Kobayashi K, Itou T, Observation of Current-Induced Bulk Magnetization in Elemental Tellurium. *Nat. Commun.* 2017;8(1):954.
- (75) Inui A, Aoki R, Nishiue Y, Shiota K, Kousaka Y, Shishido H, Hirobe D, Suda M, Ohe J, Kishine J, Yamamoto H M, Togawa Y, Chirality-Induced Spin-Polarized State of a Chiral Crystal CrNb<sub>3</sub>S<sub>6</sub>. *Phys. Rev. Lett.* 2020;124(16):166602.
- (76) Jiang N, Nii Y, Arisawa H, Saitoh E, Onose Y, Electric Current Control of Spin Helicity in an Itinerant Helimagnet. *Nat. Commun.* 2020;11(1):1601.